

SCALEFORMER: ITERATIVE MULTI-SCALE REFINING TRANSFORMERS FOR TIME SERIES FORECASTING

Mohammad Amin Shabani,
 Simon Fraser University, Canada
 & Borealis AI, Canada
 mshabani@sfu.ca

Amir Abdi, Lili Meng, Tristan Sylvain
 Borealis AI, Canada
 {firstname.lastname}@borealisai.com

ABSTRACT

The performance of time series forecasting has recently been greatly improved by the introduction of transformers. In this paper, we propose a general multi-scale framework that can be applied to the state-of-the-art transformer-based time series forecasting models (FEDformer, Autoformer, etc.). By iteratively refining a forecasted time series at multiple scales with shared weights, introducing architecture adaptations, and a specially-designed normalization scheme, we are able to achieve significant performance improvements, from 5.5% to 38.5% across datasets and transformer architectures, with minimal additional computational overhead. Via detailed ablation studies, we demonstrate the effectiveness of each of our contributions across the architecture and methodology. Furthermore, our experiments on various public datasets demonstrate that the proposed improvements outperform their corresponding baseline counterparts. Our code is publicly available in <https://github.com/BorealisAI/scaleformer>.

1 INTRODUCTION

Integrating information at different time scales is essential to accurately model and forecast time series. From weather patterns that fluctuate both locally and globally, as well as throughout the day and across seasons, to radio carrier waves which contain relevant signals at different frequencies, time series forecasting models need to encourage *scale awareness* in learnt representations. While transformer-based architectures have become the mainstream and state-of-the-art for time series forecasting in recent years, advances have focused mainly on mitigating the standard quadratic complexity in time and space, e.g., attention (Li et al., 2019; Zhou et al., 2021) or structural changes (Xu et al., 2021; Zhou et al., 2022b), rather than explicit scale-awareness. The essential cross-scale feature relationships are often learnt implicitly, and are not encouraged by architectural priors of any kind beyond the stacked attention blocks that characterize the transformer models. Autoformer (Xu et al., 2021) and Fedformer (Zhou et al., 2022b) introduced some emphasis on scale-awareness by enforcing different computational paths for the trend and seasonal components of the input time series; however, this structural prior only focused on two scales: low- and high-frequency components. **Given their importance to forecasting, can we make transformers more scale-aware?**

We enable this scale-awareness with *Scaleformer*. In our proposed approach, showcased in Figure 1, time series forecasts are iteratively refined at successive time-steps, allowing the model to better capture the inter-dependencies and specificities of each scale. However, scale itself is not sufficient. Iterative refinement at different scales can cause significant distribution shifts between intermediate

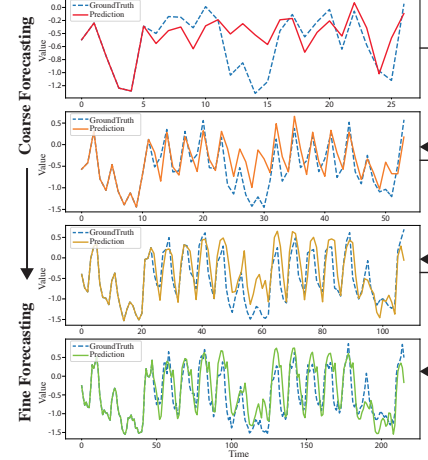


Figure 1: Intermediate forecasts by our model at different time scales. Iterative refinement of a time series forecast is a strong structural prior that benefits time series forecasting.

forecasts which can lead to runaway error propagation. To mitigate this issue, we introduce cross-scale normalization at each step.

Our approach re-orders model capacity to shift the focus on scale awareness, but does not fundamentally alter the attention-driven paradigm of transformers. As a result, it can be readily adapted to work jointly with multiple recent time series transformer architectures, acting broadly orthogonally to their own contributions. Leveraging this, we chose to operate with various transformer-based backbones (e.g. Fedformer, Autoformer, Informer, Reformer, Performer) to further probe the effect of our multi-scale method on a variety of experimental setups.

Our contributions are as follows: (1) we introduce a novel iterative scale-refinement paradigm that can be readily adapted to a variety of transformer-based time series forecasting architectures. (2) To minimize distribution shifts between scales and windows, we introduce cross-scale normalization on outputs of the Transformer. (3) Using Informer and AutoFormer, two state-of-the-art architectures, as backbones, we demonstrate empirically the effectiveness of our approach on a variety of datasets. Depending on the choice of transformer architecture, our multi-scale framework results in mean squared error reductions ranging from 5.5% to 38.5%. (4) Via a detailed ablation study of our findings, we demonstrate the validity of our architectural and methodological choices.

2 RELATED WORKS

Time-series forecasting: Time-series forecasting plays an important role in many domains, including: weather forecasting (Murphy, 1993), inventory planning (Syntetos et al., 2009), astronomy (Scargle, 1981), economic and financial forecasting (Krollner et al., 2010). One of the specificities of time series data is the need to capture *seasonal* trends (Brockwell & Davis, 2009). There exists a vast variety of time-series forecasting models (Box & Jenkins, 1968; Hyndman et al., 2008; Salinas et al., 2020; Rangapuram et al., 2018; Bai et al., 2018; Wu et al., 2020). Early approaches such as ARIMA (Box & Jenkins, 1968) and exponential smoothing models (Hyndman et al., 2008) were followed by the introduction of neural network based approaches involving either Recurrent Neural Networks (RNNs) and their variants (Salinas et al., 2020; Rangapuram et al., 2018; Salinas et al., 2020) or Temporal Convolutional Networks (TCNs) (Bai et al., 2018).

More recently, time-series Transformers (Wu et al., 2020; Zerveas et al., 2021) were introduced for the forecasting task by leveraging self-attention mechanisms to learn complex patterns and dynamics from time series data. Binh and Matteson (Tang & Matteson, 2021) proposes a probabilistic, non-auto-regressive transformer-based model with the integration of state space models. The original quadratic complexity in time and memory was lowered to $O(L \log L)$ by enforcing sparsity in the attention mechanism with the ProbSparse attention of the Informer model (Zhou et al., 2021), and the logSparse attention mechanism (Li et al., 2019). While such attention mechanisms operate on a point-wise basis, Autoformer (Xu et al., 2021) used a cross-correlation-based attention mechanism to operate at the level of subsequences. FEDformer (Zhou et al., 2022b) employs frequency transform to decompose the sequence into multiple frequency domain modes to extract the feature, further improving the performance of Autoformer.

Multi-scale neural architectures: Multi-scale and hierarchical processing is useful in many domains, such as computer vision (Fan et al., 2021; Zhang et al., 2021; Liu et al., 2018), natural language processing (Nawrot et al., 2021; Subramanian et al., 2020; Zhao et al., 2021) and time series forecasting (Chen et al., 2022; Ding et al., 2020). Multiscale Vision Transformers (Fan et al., 2021) is proposed for video and image recognition, by connecting the seminal idea of multiscale feature hierarchies with transformer models, however, it focuses on the spatial domain, specially designed for computer vision tasks. Cui et al. (2016) proposed to use different transformations of a time series such as downsampling and smoothing in parallel to the original signal to better capture temporal patterns and reduce the effect of random noise. Many different architectures have been proposed recently (Chung et al., 2016; Che et al., 2018; Shen et al., 2020; Chen et al., 2021) to improve RNNs in tasks such as language processing, computer vision, time-series analysis, and speech recognition. However, these methods are mainly focused on proposing a new RNN-based module which is not applicable to transformers directly. The same direction has been also investigated in Transformers, TCN, and MLP models. In the most recent work, Du et al. (2022) proposed multi-scale segment-wise correlations as a multi-scale version of the self-attention mechanism. Our work is orthogonal to the

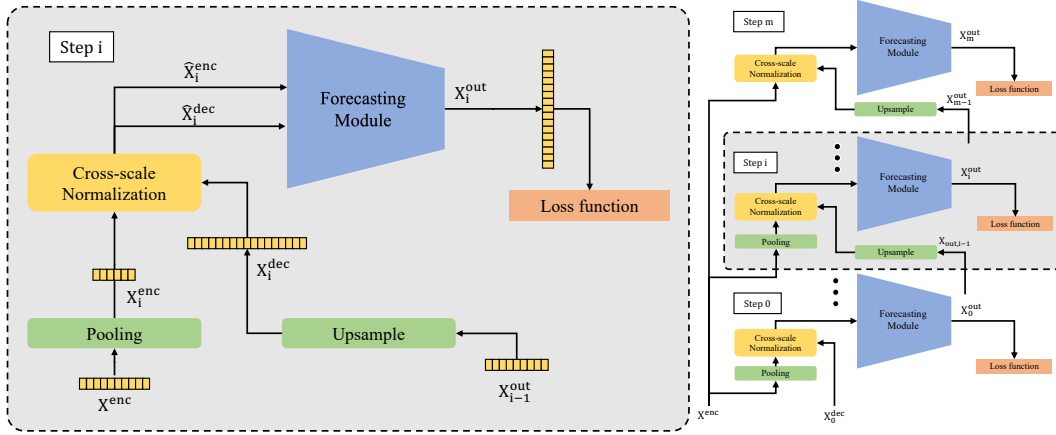


Figure 2: Overview of the proposed *Scaleformer* framework. (Left) Representation of a single scale block. In each step, we pass the normalized upsampled output from previous step along with the normalized downsampled encoder as the input. (Right) Representation of the full architecture. We process the input in a multi-scale manner iteratively from the smallest scale to the original scale.

above methods as a model-agnostic framework to utilize multi-scale time-series in transformers while keeping the number of parameters and time complexity roughly the same.

3 METHOD

In this section, we first introduce the problem setting in Sec. 3.1, then describe the proposed framework in Sec. 3.2, and the normalization scheme in Sec. 3.3. We provide details on the input’s representation in Sec. 3.4, and the loss function in Sec. 3.5.

3.1 PROBLEM SETTING

We denote $\mathbf{X}^{(L)}$ and $\mathbf{X}^{(H)}$ the look-back and horizon windows for the forecast, respectively, of corresponding lengths ℓ_L, ℓ_H . Given a starting time t_0 we can express these time-series of dimension d_x , as follows: $\mathbf{X}^{(L)} = \{\mathbf{x}_t | \mathbf{x}_t \in \mathbb{R}^{d_x}, t \in [t_0, t_0 + \ell_L]\}$ and $\mathbf{X}^{(H)} = \{\mathbf{x}_t | \mathbf{x}_t \in \mathbb{R}^{d_x}, t \in [t_0 + \ell_L + 1, t_0 + \ell_L + \ell_H]\}$. The goal of the forecasting task is to predict the horizon window $\mathbf{X}^{(H)}$ given the look-back window $\mathbf{X}^{(L)}$.

3.2 MULTI-SCALE FRAMEWORK

Our proposed framework applies successive transformer modules to iteratively refine a time-series forecast, at different temporal scales. The proposed framework is shown in Figure 2.

Given an input time-series $\mathbf{X}^{(L)}$, we iteratively apply the same neural module multiple times at different temporal scales. Concretely, we consider a set of scales $S = \{s^m, \dots, s^2, s^1, 1\}$ (i.e. for the default scale of $s = 2$, S is a set of consecutive powers of 2), where $m = \lfloor \log_s \ell_L \rfloor - 1$ and s is a downscaling factor. The input to the encoder at the i -th step ($0 \leq i \leq m$) is the original look-back window $\mathbf{X}^{(L)}$, downsampled by a scale factor of $s_i \equiv s^{m-i}$ via an average pooling operation. The input to the decoder, on the other hand, is \mathbf{X}_{i-1}^{out} upsampled by a factor of s via a linear interpolation.

Finally, $\mathbf{X}_0^{\text{dec}}$ is initialized to an array of 0s. The model performs the following operations:

$$\mathbf{x}_{t,i} = \frac{1}{s_i} \sum_{\tau=1}^{\tau+s_i} \mathbf{x}_\tau, \quad \tau = t \times s_i \quad (1)$$

$$\mathbf{X}_i^{(L)} = \left\{ \mathbf{x}_{t,i} \mid \frac{t_0}{s_i} \leq t \leq \frac{t_0 + \ell_L}{s_i} \right\} \quad (2)$$

$$\mathbf{X}_i^{(H)} = \left\{ \mathbf{x}_{t,i} \mid \frac{t_0 + \ell_L + 1}{s_i} \leq t \leq \frac{t_0 + \ell_L + \ell_H}{s_i} \right\}, \quad (3)$$

where $\mathbf{X}_i^{(L)}$ and $\mathbf{X}_i^{(H)}$ are the look-back and horizon windows at the i th step at time t with the scale factor of s^{m-i} and with the lengths of $\ell_{L,i}$ and $\ell_{H,i}$, respectively. Assuming $\mathbf{x}'_{t,i-1}$ is the output of the forecasting module at step $i-1$ and time t , we can define $\mathbf{X}_i^{\text{enc}}$ and $\mathbf{X}_i^{\text{dec}}$ as the inputs to the normalization:

$$\mathbf{X}_i^{\text{enc}} = \mathbf{X}_i^{(L)} \quad (4)$$

$$\mathbf{x}''_{t,i} = \mathbf{x}'_{\lfloor t/s \rfloor, i-1} + (\mathbf{x}'_{\lceil t/s \rceil, i-1} - \mathbf{x}'_{\lfloor t/s \rfloor, i-1}) \times \frac{t - \lfloor t/s \rfloor}{s} \quad (5)$$

$$\mathbf{X}_i^{\text{dec}} = \{ \mathbf{x}''_{t,i} \mid \frac{t_0 + \ell_L + 1}{s_i} \leq t \leq \frac{t_0 + \ell_L + \ell_H}{s_i} \}. \quad (6)$$

Finally, we calculate the error between $\mathbf{X}_i^{(H)}$ and $\mathbf{X}_i^{\text{out}}$ as the loss function to train the model. Please refer to Algorithm 1 for details on the sequence of operations performed during the forward pass.

Algorithm 1 Scaleformer: Iterative Multi-scale Refining Transformer

Require: input lookback window $\mathbf{X}^{(L)} \in \mathbb{R}^{\ell_L \times d_x}$, scale factor s ,
a set of scales $S = \{s^m, \dots, s^2, s^1, 1\}$, Horizon length ℓ_H , and Transformer module F .

for $i \leftarrow 0$ to m **do**

- $\mathbf{X}_i^{\text{enc}} \leftarrow \text{AvgPool}(\mathbf{X}^{(L)}, \text{window_size} = s^{m-i})$ ▷ Equation (1) and (2) of the paper
- if** $i = 0$ **then**

 - $\mathbf{X}_i^{\text{dec}} \leftarrow \left[\vec{0}^{\ell_H} \right]$

- else**

 - $\mathbf{X}_i^{\text{dec}} \leftarrow \text{Upsample}(\mathbf{X}_{i-1}^{\text{out}}, \text{scale} = s)$ ▷ Equation (5) and (6) of the paper

- end if**
- $\bar{\mu} \mathbf{x}_i \leftarrow \frac{1}{\ell_{L,i} + \ell_{H,i}} \left(\sum_{\mathbf{x}^{\text{enc}} \in \mathbf{X}_i^{\text{enc}}} \mathbf{x}^{\text{enc}} + \sum_{\mathbf{x}^{\text{dec}} \in \mathbf{X}_i^{\text{dec}}} \mathbf{x}^{\text{dec}} \right)$
- $\hat{\mathbf{X}}_i^{\text{dec}} \leftarrow \mathbf{X}_i^{\text{dec}} - \bar{\mu} \mathbf{x}_i$
- $\hat{\mathbf{X}}_i^{\text{enc}} \leftarrow \mathbf{X}_i^{\text{enc}} - \bar{\mu} \mathbf{x}_i$
- $\mathbf{X}_i^{\text{out}} \leftarrow F(\mathbf{X}_i^{\text{enc}}, \hat{\mathbf{X}}_i^{\text{dec}}) + \bar{\mu} \mathbf{x}_i$

end for

Ensure: $\mathbf{X}_i^{\text{out}}$ ▷ return the prediction at all scales

3.3 CROSS-SCALE NORMALIZATION

Given a set of input series $(\mathbf{X}_i^{\text{enc}}, \mathbf{X}_i^{\text{dec}})$, with dimensions $\ell_{L,i} \times d_x$ and $\ell_{H,i} \times d_x$, respectively for the encoder and the decoder of the transformer in i th step, we normalize each series based on the temporal average of $\mathbf{X}_i^{\text{enc}}$ and $\mathbf{X}_i^{\text{dec}}$. More formally:

$$\bar{\mu} \mathbf{x}_i = \frac{1}{\ell_{L,i} + \ell_{H,i}} \left(\sum_{\mathbf{x}^{\text{enc}} \in \mathbf{X}_i^{\text{enc}}} \mathbf{x}^{\text{enc}} + \sum_{\mathbf{x}^{\text{dec}} \in \mathbf{X}_i^{\text{dec}}} \mathbf{x}^{\text{dec}} \right) \quad (7)$$

$$\hat{\mathbf{X}}_i^{\text{dec}} = \mathbf{X}_i^{\text{dec}} - \bar{\mu} \mathbf{x}_i, \quad \hat{\mathbf{X}}_i^{\text{enc}} = \mathbf{X}_i^{\text{enc}} - \bar{\mu} \mathbf{x}_i \quad (8)$$

where $\bar{\mu} \mathbf{x}_i \in \mathbb{R}^{d_x}$ is the average over the temporal dimension of the concatenation of both look-back window and the horizon. Here, $\hat{\mathbf{X}}_i^{\text{enc}}$ and $\hat{\mathbf{X}}_i^{\text{dec}}$ are the inputs of the i th step to the forecasting module.

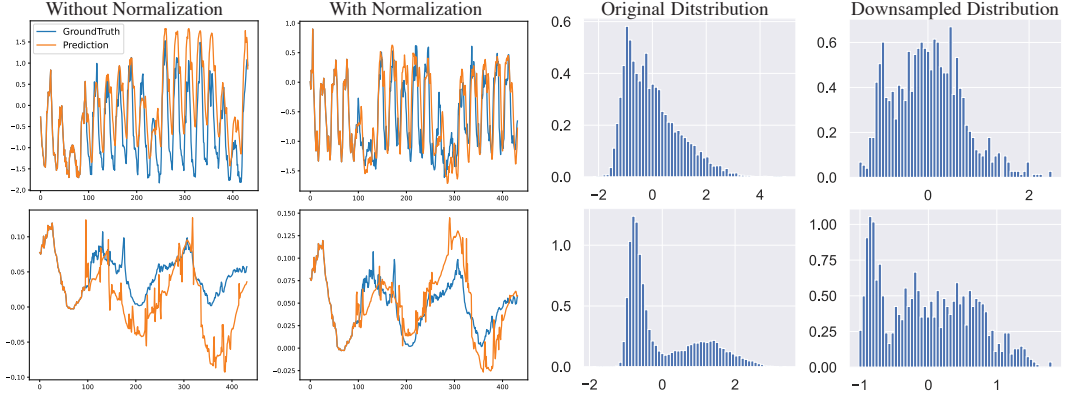


Figure 3: The figure shows the output results of two series using the same trained multi-scale model with and without shifting the data (left) which demonstrates the importance of normalization. On the right, we can see the distribution changes due to the downsampling of two series compared to the original scales from the Electricity dataset.

Distribution shift is when the distribution of input to a model or its sub-components changes across training to deployment (Shimodaira, 2000; Ioffe & Szegedy, 2015). In our context, two distinct distribution shifts are common. First, there is a natural distribution shift between the look-back window and the forecast window (the covariate shift). Additionally, there is a distribution shift between the predicted forecast windows at two consecutive scales which is a result of the upsampling operation alongside the error accumulation during the intermediate computations. As a result, normalizing the output at a given step by either the look-back window statistics or the previously predicted forecast window statistics result in an accumulation of errors across steps. We mitigate this by considering a moving average of forecast and look-back statistics as the basis for the output normalization. While this change might appear relatively minor, it has a significant impact on the resulting distribution of outputs. The improvement is more evident when compared to the alternative approaches, namely, normalizing by either look-back or previous forecast window statistics.

3.4 INPUT EMBEDDING

Following the previous works, we embed our input to have the same number of features as the hidden dimension of the model. The embedding consists of three parts: (1) *Value embedding* which uses a linear layer to map the input observations of each step x_t to the same dimension as the model. We further concatenate an additional value 0, 0.5, or 1 respectively showing if each observation is coming from the look-back window, zero initialization, or the prediction of the previous steps. (2) *Temporal Embedding* which again uses a linear layer to embed the time stamp related to each observation to the hidden dimension of the model. Here we concatenate an additional value $1/s_i - 0.5$ as the current scale for the network before passing to the linear layer. (3) We also use a fixed *positional embedding* which is adapted to the different scales s_i as follows:

$$PE(pos, 2k, s_i) = \sin\left(\frac{\text{pos} \times s_i}{10000^{2k/d_{\text{model}}}}\right), \quad PE(pos, 2k + 1, s_i) = \cos\left(\frac{\text{pos} \times s_i}{10000^{2k/d_{\text{model}}}}\right) \quad (9)$$

3.5 LOSS FUNCTION

Using the standard MSE objective to train time-series forecasting models leaves them sensitive to outliers. One possible solution is to use objectives more robust to outliers, such as the Huber loss (Huber, 1964). However, when there are no major outliers, such objectives tend to underperform. Given the heterogeneous nature of the data, we instead utilize the adaptive loss (Barron, 2019):

$$f(\xi, \alpha, c) = \frac{|\alpha - 2|}{\alpha} \left(\left(\frac{(\xi/c)^2}{|\alpha - 2|} + 1 \right)^{\alpha/2} - 1 \right) \quad (10)$$

Table 1: Comparison of the MSE and MAE results for our proposed multi-scale framework version of different methods (**-MSA**) with respective baselines. Results are given in the *multi-variate* setting, for different lengths of the horizon window. The best results are shown in **Bold**. Our method outperforms vanilla version of the baselines over almost all datasets and settings. The average improvement (error reduction) is shown in **Green** numbers at the bottom with respect the base models.

Method/ Dataset	FEDformer	FED-MSA	Autoformer	Auto-MSA	Informer	Info-MSA	Reformer	Ref-MSA	Performer	Per-MSA	
	MSE	MAE	MSE	MAE	MSE	MAE	MSE	MAE	MSE	MAE	
Exchange	96	0.155 0.285	0.109 0.240	0.154 0.285	0.126 0.259	0.966 0.792	0.168 0.298	1.063 0.826	0.182 0.311	0.667 0.669	0.179 0.305
	192	0.274 0.384	0.241 0.353	0.356 0.428	0.253 0.373	1.088 0.842	0.427 0.484	1.597 1.029	0.375 0.446	1.339 0.904	0.439 0.486
	336	0.452 0.498	0.471 0.508	0.441 0.495	0.519 0.538	1.598 1.016	0.500 0.535	1.712 1.070	0.605 0.591	1.081 0.844	0.563 0.577
	720	1.172 0.839	1.259 0.865	1.118 0.819	0.928 0.751	2.679 1.340	1.017 0.790	1.918 1.160	1.089 0.857	0.867 0.766	1.219 0.882
Weather	96	0.288 0.365	0.220 0.289	0.267 0.334	0.163 0.226	0.388 0.435	0.210 0.279	0.347 0.388	0.199 0.263	0.441 0.479	0.228 0.291
	192	0.368 0.425	0.341 0.385	0.323 0.376	0.221 0.290	0.433 0.453	0.289 0.333	0.463 0.469	0.294 0.355	0.475 0.501	0.302 0.357
	336	0.447 0.469	0.463 0.455	0.364 0.397	0.282 0.340	0.610 0.551	0.418 0.427	0.734 0.622	0.463 0.464	0.478 0.482	0.441 0.456
	720	0.640 0.574	0.682 0.565	0.425 0.434	0.369 0.396	0.978 0.723	0.595 0.532	0.815 0.674	0.493 0.471	0.563 0.552	0.817 0.655
Electricity	96	0.201 0.317	0.182 0.297	0.197 0.312	0.188 0.303	0.344 0.421	0.203 0.315	0.294 0.382	0.183 0.291	0.294 0.387	0.190 0.300
	192	0.200 0.314	0.188 0.300	0.219 0.329	0.197 0.310	0.344 0.426	0.219 0.331	0.331 0.409	0.194 0.304	0.303 0.400	0.200 0.310
	336	0.214 0.330	0.210 0.324	0.263 0.359	0.224 0.333	0.358 0.440	0.253 0.360	0.361 0.428	0.209 0.321	0.331 0.416	0.209 0.322
	720	0.239 0.350	0.232 0.339	0.290 0.380	0.249 0.358	0.386 0.452	0.293 0.390	0.316 0.393	0.234 0.340	0.304 0.386	0.228 0.335
Traffic	96	0.601 0.376	0.564 0.351	0.628 0.393	0.567 0.350	0.748 0.426	0.597 0.369	0.698 0.386	0.615 0.377	0.730 0.405	0.612 0.371
	192	0.603 0.379	0.570 0.349	0.634 0.401	0.589 0.360	0.772 0.436	0.655 0.399	0.694 0.378	0.613 0.367	0.698 0.387	0.608 0.368
	336	0.602 0.375	0.576 0.349	0.619 0.385	0.609 0.383	0.863 0.493	0.761 0.455	0.695 0.377	0.617 0.360	0.678 0.370	0.604 0.356
	720	0.615 0.378	0.602 0.360	0.656 0.403	0.642 0.397	1.074 0.606	0.924 0.521	0.692 0.376	0.638 0.360	0.672 0.364	0.634 0.360
ILI	24	3.025 1.189	2.745 1.075	3.862 1.370	3.370 1.213	5.402 1.581	3.742 1.252	3.961 1.289	3.534 1.212	4.806 1.471	3.437 1.148
	32	3.034 1.201	2.748 1.072	3.871 1.379	3.088 1.164	5.296 1.587	3.807 1.272	4.022 1.311	3.652 1.235	4.669 1.455	4.055 1.248
	48	2.444 1.041	2.793 1.059	2.891 1.138	3.207 1.153	5.226 1.569	3.940 1.272	4.269 1.340	3.506 1.168	4.488 1.371	4.055 1.248
	64	2.686 1.112	2.678 1.071	3.164 1.223	2.954 1.112	5.304 1.578	3.670 1.234	4.370 1.385	3.487 1.177	4.607 1.404	3.828 1.224
Vs Ours			5.6% 5.9%		13.5% 9.1%		38.5% 26.7%		38.3% 25.2%		23.3% 16.9%

with $\xi = (\mathbf{X}_i^{\text{out}} - \mathbf{X}_i^{(H)})$ in step i . The parameters α and c , which modulate the loss sensitivity to outliers, are learnt in an end-to-end fashion during training. To the best of our knowledge, this is the first time this objective has been adapted to the context of time-series forecasting.

4 EXPERIMENTS

In this section, we first showcase the main results of our proposed approach on a variety of forecasting dataset in Sec. 4.1. Then, we provide an ablation study of the different components of our model in Sec. 4.2, and also present qualitative results in Sec. 4.3. Moreover, we discuss a series of additional extensions of our method in Sec. 4.4, shedding light on promising future directions.

4.1 MAIN RESULTS

Baselines: To measure the effectiveness of the proposed framework, we mainly use state-of-the-art transformer-based models FedFormer (Zhou et al., 2022b) Reformer (Kitaev et al., 2020), Performer (Choromanski et al., 2020), Informer (Zhou et al., 2021) and Autoformer (Xu et al., 2021) which are proven to have beaten other transformer-based (e.g. LogTrans (Li et al., 2019), Reformer (Kitaev et al., 2020)), RNN-based (e.g. LSTMNet (Lai et al., 2018), LSTM) and TCN (Bai et al., 2018) models. For brevity, we only keep comparisons with the transformer models in the tables.

Datasets: We consider four public datasets with different characteristics to evaluate our proposed framework. **Electricity Consuming Load (ECL)**¹ corresponds to the electricity consumption (Kwh) of 321 clients. **Traffic**² aggregates the hourly occupancy rate of 963 car lanes of San Francisco bay area freeways. **Weather**³ contains 21 meteorological indicators, such as air temperature, humidity, etc, recorded every 10 minutes for the entirety of 2020. **Exchange-Rate** (Lai et al., 2018) collects the daily exchange rates of 8 countries (Australia, British, Canada, Switzerland, China, Japan, New Zealand and Singapore) from 1990 to 2016. **National Illness (ILI)**⁴ corresponds to the weekly

¹<https://archive.ics.uci.edu/ml/datasets/ElectricityLoadDiagrams20112014>

²<https://pems.dot.ca.gov>

³<https://www.bgc-jena.mpg.de/wetter>

⁴<https://gis.cdc.gov/grasp/fluview/fluportaldashboard.html>

Table 2: Multi-scale framework without cross-scale normalization. Correctly normalizing across different scales (as per our cross-mean normalization) is essential to obtain good performance when using the multi-scale framework.

Dataset	FEDformer		FED-MS (w/o N)		Autoformer		Auto-MS (w/o N)		Informer		Info-MS (w/o N)		
	Metric	MSE	MAE	MSE	MAE	MSE	MAE	MSE	MAE	MSE	MAE	MSE	MAE
Weather	96	0.288	0.365	0.300	0.342	0.267	0.334	0.191	0.277	0.388	0.435	0.402	0.438
	192	0.368	0.425	0.424	0.422	0.323	0.376	0.281	0.360	0.433	0.453	0.393	0.434
	336	0.447	0.469	0.531	0.493	0.364	0.397	0.376	0.420	0.610	0.551	0.566	0.528
	720	0.640	0.574	0.714	0.576	0.425	0.434	0.439	0.465	0.978	0.723	1.293	0.845
Electricity	96	0.201	0.317	0.258	0.356	0.197	0.312	0.221	0.337	0.344	0.421	0.407	0.465
	192	0.200	0.314	0.259	0.357	0.219	0.329	0.251	0.357	0.344	0.426	0.407	0.469
	336	0.214	0.330	0.268	0.364	0.263	0.359	0.288	0.380	0.358	0.440	0.392	0.461
	720	0.239	0.350	0.285	0.368	0.290	0.380	0.309	0.397	0.386	0.452	0.391	0.453

recorded influenza-like illness patients from the US Center for Disease Control and Prevention. We consider horizon lengths of 24, 32, 48, and 64 with an input length of 32.

Implementation details: Following previous work (Xu et al., 2021; Zhou et al., 2021), we pass $\mathbf{X}^{\text{enc}} = \mathbf{X}^{(L)}$ as the input to the encoder. While an array of zero-values would be the default to pass to the decoder, the decoder instead takes as input the second half of the look-back window padded with zeros $\mathbf{X}^{\text{dec}} = \{\mathbf{x}_{t_0+\ell_L/2}, \dots, \mathbf{x}_{\ell_L}, 0, 0, \dots, 0\}$ with length $\ell_L/2 + \ell_H$. The hidden dimension of models is 512 with a batch size of 32. We use the Adam optimizer with a learning rate of 1e-4. The look-back window size is fixed to 96, and the horizon is varied from 96 to 720. We repeat each experiment 5 times and report average values to reduce randomness. For additional implementation details on our model and baselines please refer to Appendix A.

Main results and comparison with baselines: Table 1 shows the results of the proposed framework compared to the baselines. Our proposed multi-scale framework with the adaptive loss outperforms the baselines in almost all of the experiments with an average improvement of 5.6% over FEDFormer, 13% over Autoformer and 38% over Informer which are the three most recent transformer-based architectures on MSE. We also achieved significant error reduction on MAE. The improvement is statistically significant in all cases, and in certain cases quite substantial. In particular for the exchange-rate dataset, with Informer and Reformer base models, our approach improves upon the respective baselines by over 50% averaged over the different horizon lengths.

Time and memory complexity: The proposed framework uses the same number of parameters for the model as the baselines (except two parameters α and c of the Adaptive loss). Our framework sacrifices a small amount of computation efficiency for the sake of a significant performance improvement. We expand our analysis in Appendix B. As shown in Table 4 in Appendix, if we replace the operation at the final scale by an interpolation of the prior output, we can achieve improved performance over the baselines, at no computational overhead.

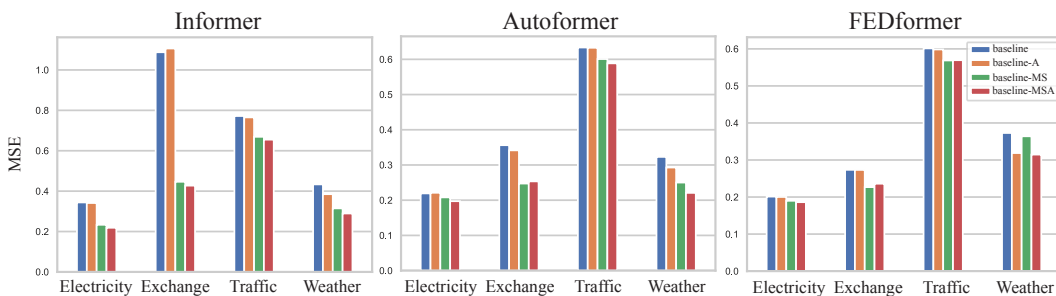


Figure 4: Comparison of training with Adaptive loss ”-A”, multi-scale framework with MSE loss ”-MS”, Multi-scale framework and Adaptive loss ”-MSA”. It shows the combination of all our proposed contributions is essential, and results in significantly improved performance.

Table 3: Single-scale framework with cross scale normalization ”-N”. The cross-scale normalization (which in the single-scale case corresponds to mean-normalization of the output) does not improve the performance of the Autoformer, as it already has an internal trend-cycle normalization component. However, it does improve the results of the Informer and FEDformer.

Dataset	FEDformer				FEDformer-N				Autoformer				Autoformer-N				Informer		Informer-N		
	Metric		MSE	MAE	Metric		MSE	MAE	Metric		MSE	MAE	Metric		MSE	MAE	Metric		MSE	MAE	
Weather	96	0.288	0.365	0.234	0.292	0.267	0.334	0.323	0.401	0.388	0.435	0.253	0.333	0.357	0.408	0.453	0.453	0.357	0.408	0.453	0.461
	192	0.368	0.425	0.287	0.337	0.323	0.376	0.531	0.543	0.433	0.453	0.433	0.453	0.453	0.453	0.453	0.453	0.453	0.453	0.453	0.461
	336	0.447	0.469	0.436	0.443	0.364	0.397	0.859	0.708	0.610	0.551	0.459	0.461	0.459	0.461	0.459	0.461	0.459	0.461	0.459	0.461
	720	0.640	0.574	0.545	0.504	0.425	0.434	1.682	1.028	0.978	0.723	0.870	0.676	0.870	0.676	0.870	0.676	0.870	0.676	0.870	0.676
Electricity	96	0.201	0.317	0.194	0.307	0.197	0.312	0.251	0.364	0.344	0.421	0.247	0.356	0.247	0.356	0.247	0.356	0.247	0.356	0.247	0.356
	192	0.200	0.314	0.195	0.304	0.219	0.329	0.263	0.372	0.344	0.426	0.291	0.394	0.291	0.394	0.291	0.394	0.291	0.394	0.291	0.394
	336	0.214	0.330	0.200	0.310	0.263	0.359	0.276	0.388	0.358	0.440	0.321	0.416	0.321	0.416	0.321	0.416	0.321	0.416	0.321	0.416
	720	0.239	0.350	0.225	0.332	0.290	0.380	0.280	0.385	0.386	0.452	0.362	0.434	0.362	0.434	0.362	0.434	0.362	0.434	0.362	0.434

4.2 ABLATION STUDY

We present main ablation studies in this section, more ablation results are shown in Appendix C.

Impact of each component: Two important components of our approach are the multi-scale framework and the use of the adaptive loss. We conduct multiple experiments (1) removing the multi-scale framework and/or (2) replacing the Adaptive loss by the MSE for training, in order to demonstrate the benefits of these two components. Figure 4 shows the effect of multi-scale and the loss function with different base models. Considering the impact of ablating the adaptive loss, we can see that for both the multi-scale and base models, training with the adaptive loss improves performance. Similarly, adding the multi-scale framework improves performance, both with and without the adaptive loss. Overall, combining the adaptive loss with the multi-scale framework results in the best performance.

Cross-scale normalization: As we discussed in Section 3.3, having the cross-scale normalization is crucial to avoid the distribution shifts. To confirm that, we conduct two experiments. Firstly, we use the multi-scale framework without the cross-scale normalization to argue that the error accumulation and covariate shift between the scales leads higher error compared to only a single scale. As shown in Table 2, while the multi-scale framework can get better results in a few cases, it mostly have higher errors than baselines.

On the other hand, adding the normalization with only a single scale can still help to achieve better performance by reducing the effect of covariate shift between the training and the test series. As shown in Table 3, the normalization improves the results of Informer and FEDformer consistently. The decomposition layer of the Autoformer solves a similar problem and replacing that with our normalization harms the capacity of the model.

4.3 QUALITATIVE RESULTS

We have also shown the qualitative comparisons between the vanilla Informer and FEDformer versus the results of our framework in Figure 5. Most notably, in both cases our approach appears significantly better at forecasting the statistical properties (such as local variance) of the signal. For more qualitative results, please refer to Section D in the Appendix.

4.4 EXTENSIONS AND DISCUSSION

The Scaleformer structural prior has been shown to be beneficial when applied to transformer-based, deterministic time series forecasting. It is not however limited to those settings. In this section, we show it can be extended to *probabilistic forecasting* and non transformer-based encoders, both of which are closely coupled with our primary application. We also aim to highlight potential promising future directions.

We show that our Scaleformer can improve performance in a probabilistic forecasting setting (please refer to Table 9 in Appendix for more details). We adopt the probabilistic output of DeepAR (Salinas et al., 2020), which is the most common probabilistic forecasting treatment. In this setting, instead

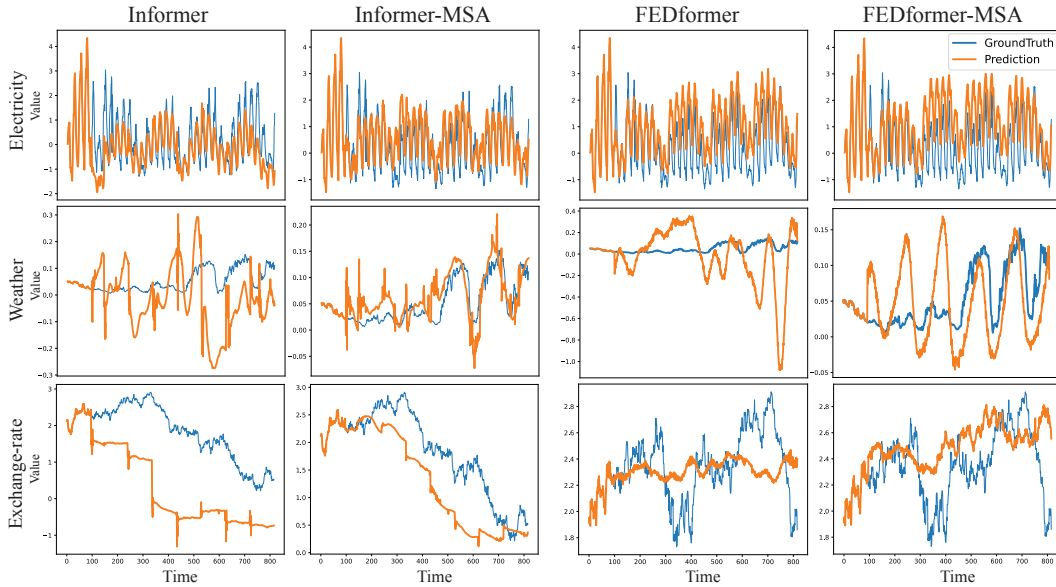


Figure 5: Qualitative comparison of base models with our framework. Our multi-scale models can better capture the global trend and local variations of the signal than their baseline equivalents. To keep the figure concise and readable, we only show Informer and FEDformer, please refer to Figure 8 in Appendix for more results.

of a point estimate, we have two prediction heads, predicting the mean μ and standard deviation σ , trained with a negative log likelihood loss (NLL). NLL and continuous ranked probability score (CRPS) are used as evaluation metrics. All other hyperparameters remain unchanged. Here, again, scaleformers continue to outperform the probabilistic Informer.

While we have mainly focused on improving transformer-based models, they are not the only encoders. Recent models such as NHits (Challu et al., 2022) and FiLM (Zhou et al., 2022a) attain competitive performance, while assuming a fixed length univariate input/output. They are less flexible compared with variable length of multi-variate input/output, but result in strong performance and faster inference than transformers, making them interesting to consider. The Scaleformer prior demonstrates a statistically significant improvement, on average, when adapted by NHits and FiLM to iteratively refine predictions. For more details please refer to Appendix F.

The results mentioned above demonstrate the fact that ScaleFormer can adapt to settings distinct from point-wise time-series forecasts with transformers (the primary scope of our paper), such as probabilistic forecasts and non-transformer models. We consider such directions to therefore be promising for future work.

5 CONCLUSION

Noting that introducing structural priors that account for multi-scale information is essential for accurate time-series forecastings, this paper proposes a novel multi-scale framework on top of recent state-the-art methods for time-series forecasting using Transformers. Our framework iteratively refines a forecasted time-series at increasingly fine-grained scales, and introduces a normalization scheme that minimizes distribution shifts between scales. These contributions result in vastly improved performance over baseline transformer architectures, across a variety of settings, and qualitatively result in forecasts that better capture the trend and local variations of the target signal. Additionally, our detailed ablation study shows that the different components synergistically work together to deliver this outcome. For future work, it is promising to extend the preliminary work that has been done applying ScaleFormer architectures to both probabilistic forecasting and non-transformer models.

REFERENCES

Shaojie Bai, J. Zico Kolter, and Vladlen Koltun. An empirical evaluation of generic convolutional and recurrent networks for sequence modeling. *arXiv:1803.01271*, 2018.

Jonathan T Barron. A general and adaptive robust loss function. In *Proceedings of the IEEE/CVF Conference on Computer Vision and Pattern Recognition*, pp. 4331–4339, 2019.

George EP Box and Gwilym M Jenkins. Some recent advances in forecasting and control. *Journal of the Royal Statistical Society. Series C (Applied Statistics)*, 17(2):91–109, 1968.

Peter J Brockwell and Richard A Davis. *Time series: theory and methods*. Springer Science & Business Media, 2009.

Cristian Challu, Kin G Olivares, Boris N Oreshkin, Federico Garza, Max Mergenthaler, and Artur Dubrawski. N-hits: Neural hierarchical interpolation for time series forecasting. *arXiv preprint arXiv:2201.12886*, 2022.

Zhengping Che, Sanjay Purushotham, Guangyu Li, Bo Jiang, and Yan Liu. Hierarchical deep generative models for multi-rate multivariate time series. In *International Conference on Machine Learning*, pp. 784–793. PMLR, 2018.

Ling Chen, Donghui Chen, Zongjiang Shang, Youdong Zhang, Bo Wen, and Chenghu Yang. Multi-scale adaptive graph neural network for multivariate time series forecasting. *arXiv preprint arXiv:2201.04828*, 2022.

Zipeng Chen, Qianli Ma, and Zhenxi Lin. Time-aware multi-scale rnns for time series modeling. In *IJCAI*, 2021.

Krzesztof Choromanski, Valerii Likhoshesterov, David Dohan, Xingyou Song, Andreea Gane, Tamas Sarlos, Peter Hawkins, Jared Davis, Afroz Mohiuddin, Lukasz Kaiser, David Belanger, Lucy Colwell, and Adrian Weller. Rethinking attention with performers, 2020.

Junyoung Chung, Sungjin Ahn, and Yoshua Bengio. Hierarchical multiscale recurrent neural networks. *arXiv preprint arXiv:1609.01704*, 2016.

Zhicheng Cui, Wenlin Chen, and Yixin Chen. Multi-scale convolutional neural networks for time series classification. *arXiv preprint arXiv:1603.06995*, 2016.

Qianggang Ding, Sifan Wu, Hao Sun, Jiadong Guo, and Jian Guo. Hierarchical multi-scale gaussian transformer for stock movement prediction. In *IJCAI*, pp. 4640–4646, 2020.

Dazhao Du, Bing Su, and Zhewei Wei. Preformer: Predictive transformer with multi-scale segment-wise correlations for long-term time series forecasting. *arXiv preprint arXiv:2202.11356*, 2022.

Haoqi Fan, Bo Xiong, Karttikeya Mangalam, Yanghao Li, Zhicheng Yan, Jitendra Malik, and Christoph Feichtenhofer. Multiscale vision transformers. In *Proceedings of the IEEE/CVF International Conference on Computer Vision*, pp. 6824–6835, 2021.

Peter J. Huber. Robust Estimation of a Location Parameter. *The Annals of Mathematical Statistics*, 35(1):73 – 101, 1964. doi: 10.1214/aoms/1177703732. URL <https://doi.org/10.1214/aoms/1177703732>.

Rob Hyndman, Anne B Koehler, J Keith Ord, and Ralph D Snyder. *Forecasting with exponential smoothing: the state space approach*. Springer Science & Business Media, 2008.

Sergey Ioffe and Christian Szegedy. Batch normalization: Accelerating deep network training by reducing internal covariate shift. In *International conference on machine learning*, pp. 448–456. PMLR, 2015.

Nikita Kitaev, Lukasz Kaiser, and Anselm Levskaya. Reformer: The efficient transformer. In *International Conference on Learning Representations*, 2020. URL <https://openreview.net/forum?id=rkgNKkHtvB>.

Bjoern Krollner, Bruce J Vanstone, Gavin R Finnie, et al. Financial time series forecasting with machine learning techniques: a survey. In *ESANN*, 2010.

Guokun Lai, Wei-Cheng Chang, Yiming Yang, and Hanxiao Liu. Modeling long-and short-term temporal patterns with deep neural networks. In *The 41st International ACM SIGIR Conference on Research & Development in Information Retrieval*, pp. 95–104, 2018.

Shiyang Li, Xiaoyong Jin, Yao Xuan, Xiyu Zhou, Wenhui Chen, Yu-Xiang Wang, and Xifeng Yan. Enhancing the locality and breaking the memory bottleneck of transformer on time series forecasting. *Advances in Neural Information Processing Systems*, 32:5243–5253, 2019.

Pengju Liu, Hongzhi Zhang, Kai Zhang, Liang Lin, and Wangmeng Zuo. Multi-level wavelet-cnn for image restoration. In *Proceedings of the IEEE conference on computer vision and pattern recognition workshops*, pp. 773–782, 2018.

Allan H Murphy. What is a good forecast? an essay on the nature of goodness in weather forecasting. *Weather and forecasting*, 8(2):281–293, 1993.

Piotr Nawrot, Szymon Tworkowski, Michał Tyrolski, Łukasz Kaiser, Yuhuai Wu, Christian Szegedy, and Henryk Michalewski. Hierarchical transformers are more efficient language models. *arXiv preprint arXiv:2110.13711*, 2021.

Adam Paszke, Sam Gross, Francisco Massa, Adam Lerer, James Bradbury, Gregory Chanan, Trevor Killeen, Zeming Lin, Natalia Gimelshein, Luca Antiga, Alban Desmaison, Andreas Kopf, Edward Yang, Zachary DeVito, Martin Raison, Alykhan Tejani, Sasank Chilamkurthy, Benoit Steiner, Lu Fang, Junjie Bai, and Soumith Chintala. Pytorch: An imperative style, high-performance deep learning library. In H. Wallach, H. Larochelle, A. Beygelzimer, F. d’Alché-Buc, E. Fox, and R. Garnett (eds.), *Advances in Neural Information Processing Systems 32*, pp. 8024–8035. Curran Associates, Inc., 2019. URL <http://papers.neurips.cc/paper/9015-pytorch-an-imperative-style-high-performance-deep-learning-library.pdf>.

Syama Sundar Rangapuram, Matthias W Seeger, Jan Gasthaus, Lorenzo Stella, Yuyang Wang, and Tim Januschowski. Deep state space models for time series forecasting. *Advances in neural information processing systems*, 31, 2018.

David Salinas, Valentin Flunkert, Jan Gasthaus, and Tim Januschowski. Deepar: Probabilistic forecasting with autoregressive recurrent networks. *International Journal of Forecasting*, 36(3): 1181–1191, 2020.

Jeffery D Scargle. Studies in astronomical time series analysis. i-modeling random processes in the time domain. *The Astrophysical Journal Supplement Series*, 45:1–71, 1981.

Lifeng Shen, Zuocong Li, and James Kwok. Timeseries anomaly detection using temporal hierarchical one-class network. *Advances in Neural Information Processing Systems*, 33:13016–13026, 2020.

Hidetoshi Shimodaira. Improving predictive inference under covariate shift by weighting the log-likelihood function. *Journal of statistical planning and inference*, 90(2):227–244, 2000.

Sandeep Subramanian, Ronan Collobert, Marc’Aurelio Ranzato, and Y-Lan Boureau. Multi-scale transformer language models. *arXiv preprint arXiv:2005.00581*, 2020.

Aris A Syntetos, John E Boylan, and Stephen M Disney. Forecasting for inventory planning: a 50-year review. *Journal of the Operational Research Society*, 60(1):S149–S160, 2009.

Binh Tang and David S Matteson. Probabilistic transformer for time series analysis. *Advances in Neural Information Processing Systems*, 34:23592–23608, 2021.

Neo Wu, Bradley Green, Xue Ben, and Shawn O’Banion. Deep transformer models for time series forecasting: The influenza prevalence case. *arXiv preprint arXiv:2001.08317*, 2020.

Jiehui Xu, Jianmin Wang, Mingsheng Long, et al. Autoformer: Decomposition transformers with auto-correlation for long-term series forecasting. *Advances in Neural Information Processing Systems*, 34, 2021.

George Zerveas, Srideepika Jayaraman, Dhaval Patel, Anuradha Bhamidipaty, and Carsten Eickhoff. A transformer-based framework for multivariate time series representation learning. In *Proceedings of the 27th ACM SIGKDD Conference on Knowledge Discovery & Data Mining*, pp. 2114–2124, 2021.

Pengchuan Zhang, Xiyang Dai, Jianwei Yang, Bin Xiao, Lu Yuan, Lei Zhang, and Jianfeng Gao. Multi-scale vision longformer: A new vision transformer for high-resolution image encoding. In *Proceedings of the IEEE/CVF International Conference on Computer Vision*, pp. 2998–3008, 2021.

Yucheng Zhao, Chong Luo, Zheng-Jun Zha, and Wenjun Zeng. Multi-scale group transformer for long sequence modeling in speech separation. In *Proceedings of the Twenty-Ninth International Conference on International Joint Conferences on Artificial Intelligence*, pp. 3251–3257, 2021.

Haoyi Zhou, Shanghang Zhang, Jieqi Peng, Shuai Zhang, Jianxin Li, Hui Xiong, and Wancai Zhang. Informer: Beyond efficient transformer for long sequence time-series forecasting. In *Proceedings of AAAI*, 2021.

Tian Zhou, Ziqing Ma, Qingsong Wen, Liang Sun, Tao Yao, Rong Jin, et al. Film: Frequency improved legendre memory model for long-term time series forecasting. *arXiv preprint arXiv:2205.08897*, 2022a.

Tian Zhou, Ziqing Ma, Qingsong Wen, Xue Wang, Liang Sun, and Rong Jin. FEDformer: Frequency enhanced decomposed transformer for long-term series forecasting. In *Proc. 39th International Conference on Machine Learning (ICML 2022)*, 2022b.

A IMPLEMENTATION DETAILS

Our implementation is based on the Pytorch (Paszke et al., 2019) implementation⁵ of the Autoformer and Informer (Xu et al., 2021). The hidden dimension of models are fixed to 512 with a batch size of 32, and we train each model for 10 epochs with early stop enabled. To optimize the models, an Adam optimizer has been used with a learning rate of 1e-4 for the forecasting model and 1e-3 for optimizing the adaptive loss. The forecasting module is fixed to 2 encoder layers and 1 decoder layer. The look-back window size is fixed to 96, and the horizon is varied from 96 to 720. We repeat each experiment 5 times to reduce the effect of randomness in the reported values. In all experiments, the temporal scale factor s is fixed to 2.

For Informer, we train the model without any changes as the core of our framework. However, Autoformer uses a decomposition layer at the input of the decoder and does not pass the trend series to the network, which makes the model unaware of the previous predictions. To resolve this, we pass zeros as the trend and the series without decomposition as the input to the decoder. For Reformer, we used the available implementation⁶ of the model from Xu et al. (2021). In addition, we used the pytorch library⁷ of Performer (Choromanski et al., 2020) for our performer baseline using the same parameters as our Reformer model, and finally, we use the official implementation⁸ of FEDformer (Zhou et al., 2022b) for the FEDformer model. We fixed the number of modes to 64 following the original paper and Wavelet Enhanced Structure for the core modules. To make it consistent with our other experiments, we use the moving average with the kernel size 25 as in Xu et al. (2021), however, FEDformer (Zhou et al., 2022b) is using moving average with the kernel size of 24. Our random seed is fixed to 2022 in all experiments.

⁵<https://github.com/thuml/Autoformer>

⁶<https://github.com/thuml/Autoformer/blob/main/models/Reformer.py>

⁷<https://github.com/lucidrains/performer-pytorch>

⁸<https://github.com/MAZiqing/FEDformer>

Table 4: Quantitative comparison of training and the test time of different experiments. Using a scale factor 2 the Scaleformer version of the baselines (showed by **-MSA**) should takes roughly twice of the original baseline time which is almost the same in the quantitative comparisons.

Method	Training time (s)				Test time (s)			
	96	192	336	720	96	192	336	720
Informer	11.38	13.83	17.38	25.31	0.79	1.12	1.21	1.23
Informer-MSA	28.73	31.88	36.37	51.15	2.42	2.63	2.87	2.96
Autoformer	17.34	23.34	31.35	52.34	1.94	2.29	2.88	3.38
Autoformer-MSA	40.57	51.17	63.53	111.84	5.22	6.06	7.04	8.10

B REDUCING COMPUTATIONAL COST

To obtain an estimation of the total running time of Scaleformer, the running time of each scale as the terms of a geometric progression based on the scale factor s which results the total time of $\frac{1-s^m}{1-s}$ multiplied by the running time of the baseline method. In this regard, Table 4 shows the running times of different experiments where $s = 2$ with the batch size is 32 on a GeForce GTX 1080 Ti GPU with 64 cores. While our current code is not optimised, still the scaleformer of each method takes roughly twice of the baselines which is consistent with the mentioned formula. Note that this is the smallest scale which means that our method is bounded to twice of the baseline and considering a larger scale factor can reduce the time overhead.

Table 5 shows the impact of replacing the Scaleformer operation at the real scale by an interpolation of values of the previous scale, i.e., at scale s^0 we do not apply the transformer but rather compute the results by linear interpolation of $\mathbf{X}_{m-1}^{\text{out}}$, thereby reducing the compute cost. This lower cost alternative results in better performance than the baselines, yet worse results than the full Scaleformer. This shows that adding scale is indeed more efficient, and that there is the possibility of a trade-off between further improved performance (full Scaleformer) or improved computational efficiency (interpolated Scaleformer).

Table 5: Comparison of the MSE and MAE results for our proposed multi-scale framework version of Informer and Autoformer by removing the last step and using an interpolation instead (**-MSA_r**) with the corresponding original models as the baseline. Results are given in the *multi-variate* setting, for different lengths of the horizon window. The look-back window size is fixed to 96 for all experiments. The best results are shown in **Bold**. Our method outperforms vanilla versions of both Informer and Autoformer over almost all datasets and settings.

Dataset	Autoformer				Informer				Informer-MSA _r	
	Metric	MSE	MAE	MSE	MAE	MSE	MAE	MSE	MAE	MSE
Exchange	96	0.154 \pm 0.01	0.285 \pm 0.00	0.132 \pm 0.02	0.265 \pm 0.02	0.966 \pm 0.10	0.792 \pm 0.04	0.248 \pm 0.07	0.366 \pm 0.06	
	192	0.356 \pm 0.09	0.428 \pm 0.05	0.418 \pm 0.22	0.466 \pm 0.12	1.088 \pm 0.04	0.842 \pm 0.01	0.727 \pm 0.19	0.637 \pm 0.09	
	336	0.441 \pm 0.02	0.495 \pm 0.01	0.736 \pm 0.25	0.629 \pm 0.10	1.598 \pm 0.08	1.016 \pm 0.02	0.643 \pm 0.03	0.620 \pm 0.02	
	720	1.118 \pm 0.04	0.819 \pm 0.02	0.773 \pm 0.26	0.709 \pm 0.13	2.679 \pm 0.22	1.340 \pm 0.06	1.036 \pm 0.08	0.803 \pm 0.03	
Weather	96	0.267 \pm 0.03	0.334 \pm 0.02	0.168 \pm 0.01	0.239 \pm 0.02	0.388 \pm 0.04	0.435 \pm 0.03	0.211 \pm 0.01	0.278 \pm 0.01	
	192	0.323 \pm 0.01	0.376 \pm 0.00	0.226 \pm 0.01	0.296 \pm 0.01	0.433 \pm 0.05	0.453 \pm 0.03	0.288 \pm 0.03	0.336 \pm 0.02	
	336	0.364 \pm 0.02	0.397 \pm 0.01	0.298 \pm 0.02	0.351 \pm 0.02	0.610 \pm 0.04	0.551 \pm 0.02	0.459 \pm 0.02	0.445 \pm 0.02	
	720	0.425 \pm 0.01	0.434 \pm 0.01	0.412 \pm 0.04	0.434 \pm 0.03	0.978 \pm 0.05	0.723 \pm 0.02	0.593 \pm 0.07	0.528 \pm 0.04	
Electricity	96	0.197 \pm 0.01	0.312 \pm 0.01	0.189 \pm 0.00	0.305 \pm 0.00	0.344 \pm 0.00	0.421 \pm 0.00	0.194 \pm 0.00	0.308 \pm 0.00	
	192	0.219 \pm 0.01	0.329 \pm 0.01	0.207 \pm 0.00	0.323 \pm 0.00	0.344 \pm 0.01	0.426 \pm 0.01	0.212 \pm 0.00	0.327 \pm 0.00	
	336	0.263 \pm 0.04	0.359 \pm 0.03	0.225 \pm 0.01	0.339 \pm 0.00	0.358 \pm 0.01	0.440 \pm 0.01	0.246 \pm 0.00	0.357 \pm 0.00	
	720	0.290 \pm 0.05	0.380 \pm 0.02	0.250 \pm 0.01	0.361 \pm 0.01	0.386 \pm 0.00	0.452 \pm 0.00	0.283 \pm 0.01	0.386 \pm 0.01	
Traffic	96	0.628 \pm 0.02	0.393 \pm 0.02	0.585 \pm 0.01	0.365 \pm 0.01	0.748 \pm 0.01	0.426 \pm 0.01	0.595 \pm 0.00	0.362 \pm 0.00	
	192	0.634 \pm 0.01	0.401 \pm 0.01	0.606 \pm 0.01	0.375 \pm 0.01	0.772 \pm 0.02	0.436 \pm 0.01	0.629 \pm 0.00	0.381 \pm 0.00	
	336	0.619 \pm 0.01	0.385 \pm 0.01	0.631 \pm 0.02	0.400 \pm 0.01	0.868 \pm 0.04	0.493 \pm 0.03	0.692 \pm 0.01	0.410 \pm 0.01	
	720	0.656 \pm 0.01	0.403 \pm 0.01	0.660 \pm 0.00	0.418 \pm 0.01	1.074 \pm 0.02	0.606 \pm 0.01	0.803 \pm 0.01	0.461 \pm 0.00	

C MORE ABLATION STUDIES AND PARAMETER ANALYSIS

C.1 MORE RESULTS ON DIFFERENT COMPONENTS

Table 6 extends the results of Figure 4 of the paper to all four datasets for both Autoformer and Informer, in the multivariate setting and for the two backbones, Autoformer and Informer.

Table 6: Comparison of training with either only an Adaptive loss ”-A”, only the multi-scale framework with MSE loss ”-MS”, or the whole Multi-scale framework and Adaptive loss ”-MSA”. The results confirm that the combination of all our proposed contributions is essential, and results in significantly improved performance in both Informer and Autoformer. Experiments are done in the multi-variate setting.

Dataset		Informer		Informer-A		Informer-MS		Informer-MSA	
Metric	MSE	MAE	MSE	MAE	MSE	MAE	MSE	MAE	
Exchange	96	0.966±0.10	0.792±0.04	0.962±0.09	0.796±0.04	0.201±0.05	0.325±0.03	0.168 ±0.05	0.298 ±0.03
	192	1.088±0.04	0.842±0.01	1.106±0.03	0.853±0.01	0.446±0.14	0.502±0.07	0.427 ±0.12	0.484 ±0.06
	336	1.598±0.08	1.016±0.02	1.602±0.07	1.019±0.01	0.520±0.05	0.540±0.02	0.500 ±0.05	0.535 ±0.02
	720	2.679±0.22	1.340±0.06	2.719±0.19	1.351±0.06	0.997 ±0.08	0.783 ±0.02	1.017±0.05	0.790±0.02
Weather	96	0.388±0.04	0.435±0.03	0.342±0.03	0.382±0.02	0.249±0.02	0.324±0.01	0.210 ±0.02	0.279 ±0.02
	192	0.433±0.05	0.453±0.03	0.385±0.02	0.404±0.01	0.315±0.02	0.380±0.02	0.289 ±0.01	0.333 ±0.01
	336	0.610±0.04	0.551±0.02	0.656±0.10	0.550±0.04	0.473±0.04	0.478±0.02	0.418 ±0.04	0.427 ±0.03
	720	0.978±0.05	0.723±0.02	0.953±0.04	0.680±0.02	0.664±0.04	0.585±0.02	0.595 ±0.04	0.532 ±0.02
Electricity	96	0.344±0.00	0.421±0.00	0.321±0.00	0.402±0.00	0.211±0.00	0.326±0.00	0.203 ±0.01	0.315 ±0.01
	192	0.344±0.01	0.426±0.01	0.341±0.01	0.422±0.01	0.233±0.01	0.348±0.00	0.219 ±0.00	0.331 ±0.00
	336	0.358±0.01	0.440±0.01	0.344±0.00	0.422±0.00	0.279±0.01	0.388±0.01	0.253 ±0.01	0.360 ±0.01
	720	0.386±0.00	0.452±0.00	0.363±0.00	0.432±0.00	0.315±0.01	0.411±0.00	0.293 ±0.01	0.390 ±0.01
Traffic	96	0.748±0.01	0.426±0.01	0.744±0.02	0.413±0.01	0.602±0.01	0.375±0.01	0.597 ±0.01	0.369 ±0.00
	192	0.772±0.02	0.436±0.01	0.765±0.01	0.416±0.01	0.669±0.01	0.412±0.00	0.655 ±0.01	0.399 ±0.01
	336	0.868±0.04	0.493±0.03	0.852±0.05	0.461±0.03	0.815±0.03	0.501±0.02	0.761 ±0.03	0.455 ±0.03
	720	1.074±0.02	0.606±0.01	1.030±0.05	0.539±0.03	0.949±0.01	0.556±0.02	0.924 ±0.02	0.521 ±0.01
Dataset		Autoformer		Autoformer-A		Autoformer-MS		Autoformer-MSA	
Metric	MSE	MAE	MSE	MAE	MSE	MAE	MSE	MAE	
Exchange	96	0.154±0.01	0.285±0.00	0.152±0.01	0.282±0.00	0.145±0.02	0.276±0.01	0.126 ±0.01	0.259 ±0.01
	192	0.356±0.09	0.428±0.05	0.342±0.10	0.421±0.06	0.247 ±0.02	0.366 ±0.01	0.253±0.03	0.373±0.02
	336	0.441 ±0.02	0.495 ±0.01	0.566±0.22	0.554±0.10	0.456±0.08	0.514±0.05	0.519±0.16	0.538±0.09
	720	1.118±0.04	0.819±0.02	1.120±0.24	0.811±0.10	0.729 ±0.16	0.679 ±0.08	0.928±0.23	0.751±0.09
Weather	96	0.267±0.03	0.334±0.02	0.229±0.01	0.288±0.01	0.174±0.01	0.254±0.01	0.163 ±0.01	0.226 ±0.01
	192	0.323±0.01	0.376±0.00	0.293±0.02	0.340±0.02	0.250±0.02	0.333±0.02	0.221 ±0.01	0.290 ±0.02
	336	0.364±0.02	0.397±0.01	0.357±0.01	0.387±0.01	0.314±0.02	0.380±0.02	0.282 ±0.02	0.340 ±0.03
	720	0.425±0.01	0.434±0.01	0.419±0.01	0.422±0.01	0.414±0.03	0.457±0.02	0.369 ±0.04	0.396 ±0.03
Electricity	96	0.197±0.01	0.312±0.01	0.201±0.01	0.312±0.01	0.196±0.00	0.312±0.01	0.188 ±0.00	0.303 ±0.01
	192	0.219±0.01	0.329±0.01	0.221±0.01	0.328±0.01	0.208±0.00	0.323±0.00	0.197 ±0.00	0.310 ±0.00
	336	0.263±0.04	0.359±0.03	0.232±0.01	0.339±0.01	0.220 ±0.00	0.336±0.00	0.224±0.02	0.333 ±0.01
	720	0.290±0.05	0.380±0.02	0.249 ±0.01	0.351 ±0.01	0.252±0.00	0.364±0.00	0.249±0.01	0.358±0.01
Traffic	96	0.628±0.02	0.393±0.02	0.610±0.02	0.381±0.01	0.580±0.01	0.358±0.00	0.567 ±0.00	0.350 ±0.00
	192	0.634±0.01	0.401±0.01	0.633±0.02	0.396±0.02	0.601±0.00	0.369±0.00	0.589 ±0.01	0.360 ±0.01
	336	0.619±0.01	0.385±0.01	0.618 ±0.00	0.381 ±0.00	0.639±0.02	0.397±0.01	0.619±0.01	0.383±0.01
	720	0.656±0.01	0.403±0.01	0.654±0.02	0.397 ±0.01	0.680±0.02	0.427±0.01	0.642 ±0.01	0.397±0.01

C.2 ITERATIVE REFINEMENT USING THE SAME SCALE

To further confirm the effect of the multi-scale framework, we also compare our proposed framework with another baseline by keeping the original scale in each iteration. As Table 7 shows, using multi-scale framework outperforms keeping the original scale while having significantly lower memory and time complexity overhead. Following the main experiments, we use the scale factor of 2 which results $S = \{16, 8, 4, 2, 1\}$ for Scaleformer (showed by -MSA) and a scale factor of 1 with similarly 5 iterations for iterative refinement (showed by -IA).

Table 7: Comparison of the MSE and MAE results for our proposed multi-scale framework version of Informer and Autoformer (-MSA) with the iterative refinemenet baseline of keeping the original scale in each iteration (-IA)

Dataset	Autoformer-MSA				Autoformer-IA				Informer-MSA				Informer-IA				
	Metric		MSE	MAE	Metric		MSE	MAE	Metric		MSE	MAE	Metric		MSE	MAE	
Exchange	96	0.126 \pm 0.01	0.259 \pm 0.01	0.410 \pm 0.05	0.485 \pm 0.03	0.168 \pm 0.05	0.298 \pm 0.03	0.649 \pm 0.08	0.632 \pm 0.04	96	0.427 \pm 0.12	0.484 \pm 0.06	0.938 \pm 0.03	0.761 \pm 0.01	96	0.253 \pm 0.03	0.373 \pm 0.02
	192	0.221 \pm 0.01	0.290 \pm 0.02	0.809 \pm 0.14	0.698 \pm 0.06	0.210 \pm 0.02	0.279 \pm 0.02	0.222 \pm 0.01	0.286 \pm 0.02		0.289 \pm 0.01	0.333 \pm 0.01	0.357 \pm 0.02	0.393 \pm 0.02		0.188 \pm 0.00	0.303 \pm 0.01
Weather	96	0.163 \pm 0.01	0.226 \pm 0.01	0.233 \pm 0.01	0.293 \pm 0.00	0.210 \pm 0.02	0.279 \pm 0.02	0.222 \pm 0.01	0.286 \pm 0.02	96	0.197 \pm 0.00	0.310 \pm 0.00	0.248 \pm 0.01	0.237 \pm 0.00	0.237 \pm 0.00	0.203 \pm 0.01	0.315 \pm 0.01
	192	0.197 \pm 0.00	0.310 \pm 0.00	0.265 \pm 0.01	0.373 \pm 0.01	0.219 \pm 0.00	0.331 \pm 0.00	0.271 \pm 0.01	0.344 \pm 0.00		0.197 \pm 0.00	0.310 \pm 0.00	0.265 \pm 0.01	0.271 \pm 0.01	0.271 \pm 0.01	0.567 \pm 0.00	0.350 \pm 0.00
Traffic	96	0.567 \pm 0.00	0.350 \pm 0.00	0.681 \pm 0.03	0.432 \pm 0.01	0.597 \pm 0.01	0.655 \pm 0.01	0.369 \pm 0.00	0.641 \pm 0.01	96	0.589 \pm 0.01	0.360 \pm 0.01	0.699 \pm 0.02	0.446 \pm 0.01	0.695 \pm 0.01	0.367 \pm 0.01	0.388 \pm 0.01
	192	0.589 \pm 0.01	0.360 \pm 0.01	0.699 \pm 0.02	0.446 \pm 0.01	0.655 \pm 0.01	0.695 \pm 0.01	0.399 \pm 0.01	0.695 \pm 0.01		0.367 \pm 0.01	0.388 \pm 0.01	0.695 \pm 0.01	0.695 \pm 0.01	0.695 \pm 0.01	0.367 \pm 0.01	0.388 \pm 0.01

C.3 RESULTS ON DIFFERENT SCALES

Table 8 showcases the results of our model using different values of the scale parameter s . It shows that a scale of 2 results in better performance.

C.4 EFFECT OF α ON THE LOSS FUNCTION

Figure 6 shows the impact of α on the shape of the loss function on the left, and example ground truth time-series corresponding to the horizon window on the right. As noted in the main paper, lower values of α tend to result in better robustness to outliers. This is indeed confirmed empirically in the case of the weather dataset, which corresponds to the lowest learnt α value, and has the outliers with the largest relative scales. For simplicity, we have excluded c on the analysis as it does not impact the robustness with regards to the outliers, as shown in [Barron \(2019\)](#).

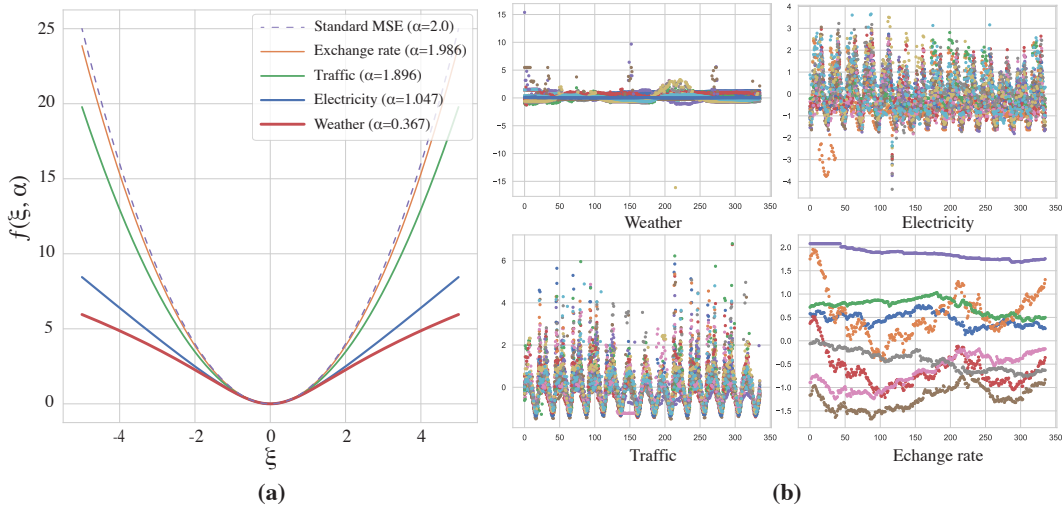


Figure 6: (a) The loss value based as a function of the ξ (absolute difference between prediction and target) and the learned α for each dataset. Different colors correspond to different datasets (each with specific value of α). (b) Samples taken from the ground-truth horizon window of each dataset. The Weather dataset sample has the outliers with the largest scales compared to the input series. As a consequence, the learnt value of α is the lowest. Different colors correspond to different variables in the multi-variate time-series we are considering.

Table 8: Comparison of the baselines with our method using different scales. Reducing the scale factor from $s = 16$ to $s = 2$ increases the number of steps but achieves lower error on average.

Dataset		Informer		Informer-MSA(s=16)		Informer-MSA(s=4)		Informer-MSA(s=2)	
Metric		MSE	MAE	MSE	MAE	MSE	MAE	MSE	MAE
Exchange	96	0.966 \pm 0.10	0.792 \pm 0.04	0.376 \pm 0.08	0.480 \pm 0.04	0.246 \pm 0.06	0.374 \pm 0.04	0.168 \pm 0.05	0.298 \pm 0.03
	192	1.088 \pm 0.04	0.842 \pm 0.01	0.878 \pm 0.08	0.721 \pm 0.03	0.661 \pm 0.20	0.617 \pm 0.09	0.427 \pm 0.12	0.484 \pm 0.06
	336	1.598 \pm 0.08	1.016 \pm 0.02	0.899 \pm 0.07	0.733 \pm 0.03	0.697 \pm 0.10	0.648 \pm 0.05	0.500 \pm 0.05	0.535 \pm 0.02
	720	2.679 \pm 0.22	1.340 \pm 0.06	1.633 \pm 0.14	1.031 \pm 0.05	1.457 \pm 0.27	0.958 \pm 0.09	1.017 \pm 0.05	0.790 \pm 0.02
Weather	96	0.388 \pm 0.04	0.435 \pm 0.03	0.208 \pm 0.02	0.275 \pm 0.02	0.189 \pm 0.01	0.259 \pm 0.01	0.210 \pm 0.02	0.279 \pm 0.02
	192	0.433 \pm 0.05	0.453 \pm 0.03	0.302 \pm 0.02	0.354 \pm 0.02	0.287 \pm 0.02	0.333 \pm 0.01	0.289 \pm 0.01	0.333 \pm 0.01
	336	0.610 \pm 0.04	0.551 \pm 0.02	0.470 \pm 0.06	0.456 \pm 0.04	0.420 \pm 0.03	0.433 \pm 0.02	0.418 \pm 0.04	0.427 \pm 0.03
	720	0.978 \pm 0.05	0.723 \pm 0.02	0.639 \pm 0.07	0.544 \pm 0.04	0.627 \pm 0.07	0.543 \pm 0.04	0.595 \pm 0.04	0.532 \pm 0.02
Electricity	96	0.344 \pm 0.00	0.421 \pm 0.00	0.215 \pm 0.00	0.329 \pm 0.00	0.203 \pm 0.00	0.315 \pm 0.00	0.203 \pm 0.01	0.315 \pm 0.01
	192	0.344 \pm 0.01	0.426 \pm 0.01	0.257 \pm 0.01	0.370 \pm 0.01	0.235 \pm 0.01	0.347 \pm 0.01	0.219 \pm 0.00	0.331 \pm 0.00
	336	0.358 \pm 0.01	0.440 \pm 0.01	0.300 \pm 0.04	0.400 \pm 0.03	0.264 \pm 0.01	0.373 \pm 0.01	0.253 \pm 0.01	0.360 \pm 0.01
	720	0.386 \pm 0.00	0.452 \pm 0.00	0.334 \pm 0.03	0.418 \pm 0.02	0.306 \pm 0.01	0.401 \pm 0.01	0.293 \pm 0.01	0.390 \pm 0.01
Traffic	96	0.748 \pm 0.01	0.426 \pm 0.01	0.648 \pm 0.02	0.386 \pm 0.01	0.616 \pm 0.00	0.374 \pm 0.01	0.597 \pm 0.01	0.369 \pm 0.00
	192	0.772 \pm 0.02	0.436 \pm 0.01	0.679 \pm 0.01	0.391 \pm 0.01	0.686 \pm 0.01	0.404 \pm 0.01	0.655 \pm 0.01	0.399 \pm 0.01
	336	0.868 \pm 0.04	0.493 \pm 0.03	0.811 \pm 0.02	0.455 \pm 0.01	0.782 \pm 0.03	0.451 \pm 0.02	0.761 \pm 0.03	0.455 \pm 0.03
	720	1.074 \pm 0.02	0.606 \pm 0.01	1.020 \pm 0.07	0.542 \pm 0.03	0.965 \pm 0.03	0.521 \pm 0.01	0.924 \pm 0.02	0.521 \pm 0.01
Dataset		Autoformer		Autoformer-MSA(16)		Autoformer-MSA(4)		Autoformer-MSA(2)	
Metric		MSE	MAE	MSE	MAE	MSE	MAE	MSE	MAE
Exchange	96	0.154 \pm 0.01	0.285 \pm 0.00	0.182 \pm 0.03	0.316 \pm 0.03	0.170 \pm 0.03	0.304 \pm 0.02	0.126 \pm 0.01	0.259 \pm 0.01
	192	0.356 \pm 0.09	0.428 \pm 0.05	0.514 \pm 0.18	0.537 \pm 0.10	0.359 \pm 0.14	0.443 \pm 0.08	0.253 \pm 0.03	0.373 \pm 0.02
	336	0.441 \pm 0.02	0.495 \pm 0.01	0.527 \pm 0.07	0.570 \pm 0.04	0.606 \pm 0.18	0.585 \pm 0.10	0.519 \pm 0.16	0.538 \pm 0.09
	720	1.118 \pm 0.04	0.819 \pm 0.02	1.019 \pm 0.18	0.819 \pm 0.08	0.973 \pm 0.22	0.809 \pm 0.09	0.928 \pm 0.23	0.751 \pm 0.09
Weather	96	0.267 \pm 0.03	0.334 \pm 0.02	0.169 \pm 0.00	0.239 \pm 0.01	0.164 \pm 0.00	0.234 \pm 0.01	0.163 \pm 0.01	0.226 \pm 0.01
	192	0.323 \pm 0.01	0.376 \pm 0.00	0.240 \pm 0.03	0.310 \pm 0.03	0.229 \pm 0.01	0.299 \pm 0.02	0.221 \pm 0.01	0.290 \pm 0.02
	336	0.364 \pm 0.02	0.397 \pm 0.01	0.304 \pm 0.03	0.354 \pm 0.03	0.303 \pm 0.01	0.350 \pm 0.01	0.282 \pm 0.02	0.340 \pm 0.03
	720	0.425 \pm 0.01	0.434 \pm 0.01	0.375 \pm 0.01	0.403 \pm 0.01	0.382 \pm 0.02	0.414 \pm 0.01	0.369 \pm 0.04	0.396 \pm 0.03
Electricity	96	0.197 \pm 0.01	0.312 \pm 0.01	0.190 \pm 0.00	0.306 \pm 0.00	0.188 \pm 0.00	0.303 \pm 0.00	0.188 \pm 0.00	0.303 \pm 0.01
	192	0.219 \pm 0.01	0.329 \pm 0.01	0.206 \pm 0.01	0.320 \pm 0.01	0.207 \pm 0.00	0.320 \pm 0.00	0.197 \pm 0.00	0.310 \pm 0.00
	336	0.263 \pm 0.04	0.359 \pm 0.03	0.236 \pm 0.02	0.344 \pm 0.01	0.237 \pm 0.03	0.344 \pm 0.02	0.224 \pm 0.02	0.333 \pm 0.01
	720	0.290 \pm 0.05	0.380 \pm 0.02	0.260 \pm 0.01	0.368 \pm 0.01	0.261 \pm 0.01	0.369 \pm 0.01	0.249 \pm 0.01	0.358 \pm 0.01
Traffic	96	0.628 \pm 0.02	0.393 \pm 0.02	0.605 \pm 0.01	0.380 \pm 0.01	0.594 \pm 0.02	0.367 \pm 0.01	0.567 \pm 0.00	0.350 \pm 0.00
	192	0.634 \pm 0.01	0.401 \pm 0.01	0.626 \pm 0.01	0.393 \pm 0.01	0.600 \pm 0.01	0.369 \pm 0.00	0.589 \pm 0.01	0.360 \pm 0.01
	336	0.619 \pm 0.01	0.385 \pm 0.01	0.635 \pm 0.01	0.400 \pm 0.00	0.625 \pm 0.01	0.386 \pm 0.01	0.619 \pm 0.01	0.383 \pm 0.01
	720	0.656 \pm 0.01	0.403 \pm 0.01	0.697 \pm 0.03	0.439 \pm 0.01	0.678 \pm 0.02	0.422 \pm 0.02	0.642 \pm 0.01	0.397 \pm 0.01

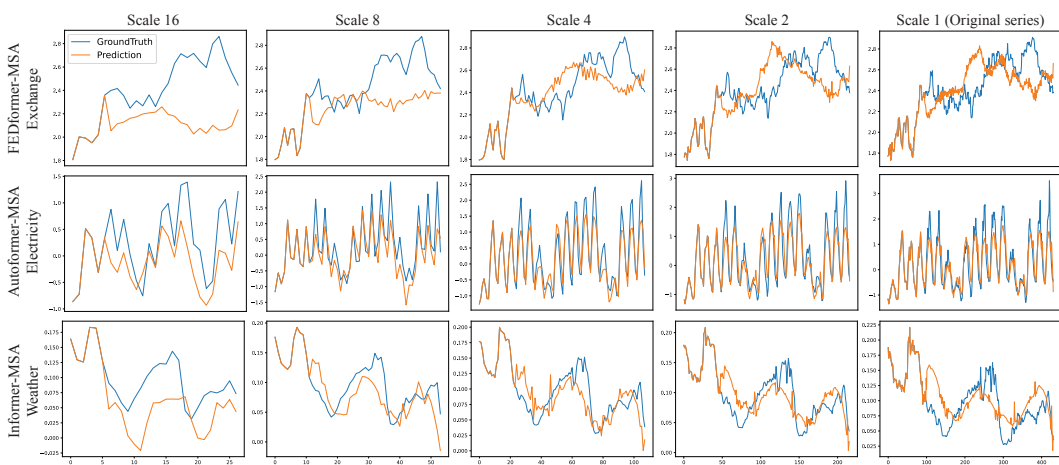


Figure 7: Qualitative results of each scale. The model can correct its previous mistakes on higher scales, showcasing increased robustness to forecasting artifacts that occur individually at each scale.

D ADDITIONAL QUALITATIVE RESULTS

Figure 7 and Figure 8 provide additional qualitative results respectively showing the intermediate results of each scale and the comparison between the baselines and our approach. As we can see, Scaleformer is able to better learn local and global time-series variations.

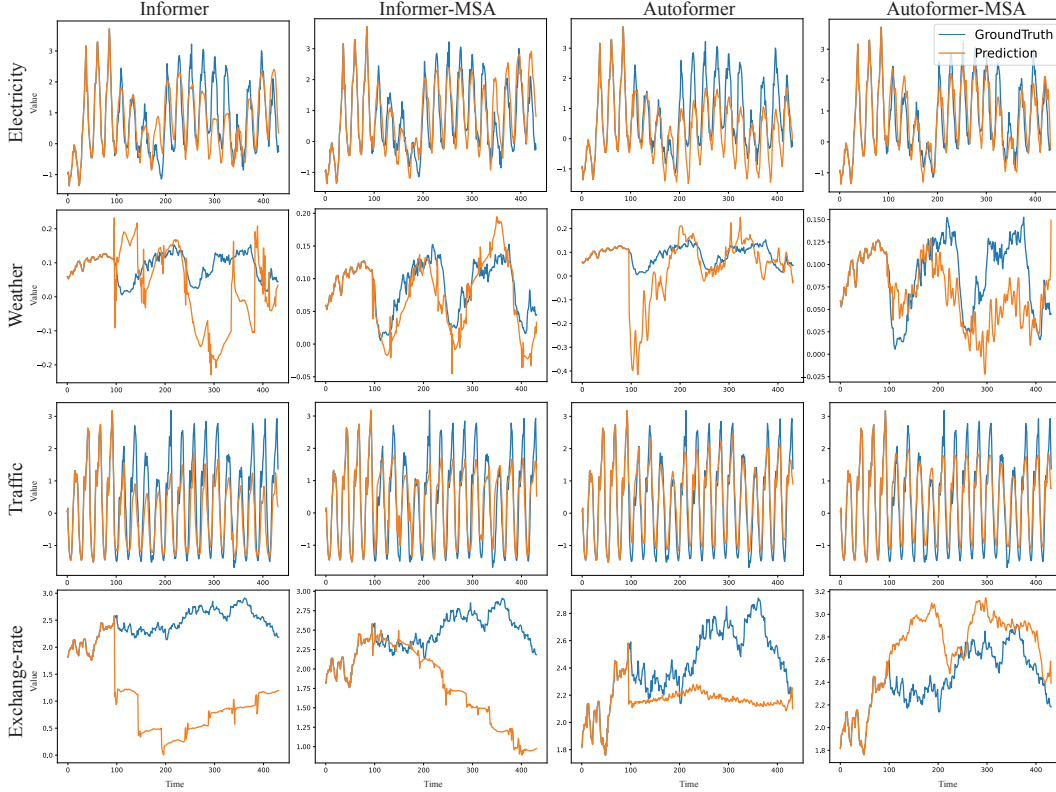


Figure 8: Additional qualitative comparison of the baselines against our framework.

E PROBABILISTIC FORECASTING

Table 9 shows the comparison of probabilistic methods for Informer by following the probabilistic output of DeepAR (Salinas et al., 2020), which is the most common probabilistic forecasting treatment.

Table 9: Scaleformer improving probabilistic metrics in Probabilistic forecasting for Informer. By adapting Informer to make probabilistic predictions, we are able to show the Scaleformer prior again brings benefits. While such an analysis excludes dedicated probabilistic approaches for conciseness, it nevertheless shows the *generality* of our proposed approach.

Dataset	Metric	96		192		336		720	
		CRPS	NLL	CRPS	NLL	CRPS	NLL	CRPS	NLL
Exchange	Informer	0.548 \pm 0.02	2.360 \pm 0.20	0.702 \pm 0.05	4.350 \pm 1.45	0.826 \pm 0.02	4.302 \pm 0.49	1.268 \pm 0.06	13.140 \pm 1.84
	Informer-MSA	0.202\pm0.01	0.452\pm0.09	0.284\pm0.02	0.818\pm0.11	0.414\pm0.06	1.724\pm0.43	0.570\pm0.03	2.862\pm0.21
Weather	Informer	0.376 \pm 0.03	1.180 \pm 0.21	0.502 \pm 0.03	1.752 \pm 0.23	0.564 \pm 0.02	1.928 \pm 0.27	0.684 \pm 0.09	2.210 \pm 0.46
	Informer-MSA	0.250\pm0.02	0.392\pm0.14	0.294\pm0.01	0.610\pm0.04	0.308\pm0.02	0.728\pm0.10	0.438\pm0.04	1.270\pm0.14
Electricity	Informer	0.330 \pm 0.01	1.106 \pm 0.05	0.338 \pm 0.05	1.254 \pm 0.04	0.348 \pm 0.01	1.244 \pm 0.07	0.528 \pm 0.00	1.856 \pm 0.06
	Informer-MSA	0.238\pm0.01	0.578\pm0.01	0.290\pm0.00	0.776\pm0.01	0.324\pm0.03	0.904\pm0.10	0.358\pm0.01	1.022\pm0.04
Traffic	Informer	0.372 \pm 0.04	1.376 \pm 0.05	0.340 \pm 0.01	1.404 \pm 0.04	0.372 \pm 0.01	1.516 \pm 0.06	0.568 \pm 0.01	1.658 \pm 0.01
	Informer-MSA	0.288\pm0.01	1.094\pm0.03	0.312\pm0.01	1.102\pm0.04	0.368\pm0.02	1.194\pm0.05	0.442\pm0.02	1.378\pm0.06

On implementation details, instead of point estimate, we have two prediction heads (one predict μ and one predict σ) with negative log likelihood loss. The other hyper parameters is the same as before. We use NLL loss and continuous ranked probability score (CRPS) which are commonly used in probabilistic forecasting as evaluation metrics.

F EXTENSION TO OTHER METHODS

Table 10 shows the comparison results of NHits (Challu et al., 2022) and FiLM (Zhou et al., 2022a) as two baselines. For each method, we copy original model to have model for different scales and we concatenate the input with the output of previous scale for the new scale. The training hyperparameters such as optimizer and learning rate is the same as the previous baselines.

Table 10: The effect of applying our proposed framework to NHits and FiLM as two non-transformer based models. Best results are shown in **Bold**.

Dataset	Metric	NHits		NHits-MSA		FiLM		FiLM-MSA	
		MSE	MAE	MSE	MAE	MSE	MAE	MSE	MAE
Exchange	96	0.091±0.00	0.218±0.01	0.087±0.00	0.206±0.00	0.083±0.00	0.201±0.00	0.081±0.00	0.197±0.00
	192	0.200±0.02	0.332±0.01	0.186±0.01	0.306±0.00	0.179±0.00	0.301±0.00	0.156±0.00	0.284±0.00
	336	0.347±0.03	0.442±0.02	0.381±0.01	0.445±0.01	0.341±0.00	0.421±0.00	0.253±0.01	0.378±0.01
	720	0.761±0.20	0.662±0.08	1.124±0.07	0.808±0.03	0.896±0.01	0.714±0.00	0.728±0.01	0.659±0.00
Weather	96	0.169±0.00	0.228±0.00	0.167±0.00	0.211±0.00	0.194±0.00	0.235±0.00	0.195±0.00	0.232±0.00
	192	0.210±0.00	0.268±0.00	0.208±0.00	0.253±0.00	0.238±0.00	0.270±0.00	0.235±0.00	0.269±0.00
	336	0.261±0.00	0.313±0.00	0.261±0.00	0.294±0.00	0.288±0.00	0.305±0.00	0.275±0.00	0.303±0.00
	720	0.333±0.01	0.372±0.01	0.331±0.00	0.348±0.00	0.359±0.00	0.350±0.00	0.337±0.00	0.356±0.00